(51) H. R. Allcock and R. J. Ritchie, to be published.
(52) M. Biddlestone and R. A. Shaw, *J. Chem. Soc. A*, 178 (1969); 1760 (1970); 2715 (1971).
(53) E. T. McBee, K. Okuhara, and C. J. Morton, *Inorg. Chem.*, **4**, 1672 (1965).
(54) A. Schmidpeter and H. Rossknecht, *Angew. Chem., Int. Ed. Engl.*, **8**, 614 (1969).
(55) At very low copper concentrations the main products of the reaction were shown by gas chromatography/mass spectrometry to consist of $N_3P_3Cl_5CH_3$ (IV) and $N_3P_3Cl_4(CH_3)_2$ (V).

Nickel–Boron "Hybrid" Clusters. Synthesis of Polyhedral Nickelaboranes and Nickelacarboranes from Small Borane and Carborane Anions. Crystal Structure of $(\eta^5\text{-}C_5H_5)_4Ni_4B_4H_4$

James R. Bowser, Alan Bonny, J. Robert Pipal, and Russell N. Grimes*

Contribution from the Department of Chemistry, University of Virginia, Charlottesville, Virginia 22901. *Received March 30, 1979*

Abstract: Insertion of two to four nickel atoms into polyborane cages has been accomplished by reactions of metal reagents with the $B_5H_8^-$ and $(CH_3)_2C_2B_4H_5^-$ ions in tetrahydrofuran followed by air oxidation. Treatment of NaB_5H_8 with $NiBr_2$ and NaC_5H_5 generates *closo*-1,6-$(\eta^5\text{-}C_5H_5)_2Ni_2B_8H_8$ and *closo*-1,7-$(\eta^5\text{-}C_5H_5)_2Ni_2B_{10}H_{10}$, and the reaction of NaB_5H_8 with $(\eta^5\text{-}C_5H_5)_2Ni$ and sodium amalgam gives *closo*-$(\eta^5\text{-}C_5H_5)_4Ni_4B_4H_4$ and *nido*-$(\eta^5\text{-}C_5H_5)_4Ni_4B_5H_5$. Nickelocene and $Na(CH_3)_2C_2B_4H_5$ yield *closo*-$(\eta^5\text{-}C_5H_5)_2Ni_2(CH_3)_2C_2B_4H_4$ and *nido*-$(\eta^5\text{-}C_5H_5)_2Ni_2(CH_3)_2C_2B_5H_5$. The new compounds were structurally characterized from their ^{11}B and ^1H pulse Fourier transform NMR, IR, and low- and high-resolution mass spectra and an X-ray crystal structure determination on $(\eta^5\text{-}C_5H_5)_4Ni_4B_4H_4$. The latter molecule has closo-D_{2d} cage geometry despite the presence of 20 skeletal valence electrons, from which a nido structure would be predicted on the basis of electron counting rules. Its analogue $(\eta^5\text{-}C_5H_5)_2Ni_2(CH_3)_2C_2B_4H_4$ also has been assigned a D_{2d} closo structure, but $(\eta^5\text{-}C_5H_5)_4Ni_4B_5H_5$ is a nido (monocapped square antiprism) cage system, and its counterpart $(\eta^5\text{-}C_5H_5)_2Ni_2(CH_3)_2C_2B_5H_5$ probably has a similar cage geometry. The Ni_4B_4 and Ni_4B_5 clusters are the second and third examples (after $(\eta^5\text{-}C_5H_5)_4Co_4B_4H_4$) of tetrametallic metalloboron cages, and are hybrid systems related to both the metal clusters and the boranes. In $(\eta^5\text{-}C_5H_5)_4Ni_4B_4H_4$ the nickel atoms occupy low-coordinate vertices in the D_{2d} polyhedron, in contrast to $(\eta^5\text{-}C_5H_5)_4Co_4B_4H_4$, where the cobalt atoms occupy the high-coordinate positions. The Ni–Ni distance of 2.354 (1) Å is the shortest known metal–metal link in any type of metalloboron polyhedron, and may indicate localized metal–metal bonding. Crystal data for $(\eta^5\text{-}C_5H_5)_4Ni_4B_4H_4$ follow: space group $C2/c$, $Z = 4$, $a = 19.546$ (4) Å, $b = 7.512$ (4) Å, $c = 14.86$ (1) Å, $\beta = 106.70$ (2)°, $V = 2090$ (2) Å^3, $R = 0.043$ for the 1500 reflections for which $F_o^2 \geqslant 3\sigma(F_o^2)$.

Metal-rich metalloboron polyhedra are compositionally intermediate between the polyhedral boranes and the metal clusters, and may be regarded as "hybrid" species which in a structural and electronic sense are members of both families.[1] The stable existence of such compounds provides concrete support for the thesis, first advanced by Wade[2] and subsequently developed by several authors,[3] that the metal cluster, organometallic cluster, and borane families are related electronically and are amenable to the same kind of molecular orbital description. This idea is the basis for the widely used electron-counting rules[3a] that correlate cage structure with framework electron population.

A continuing research interest in our laboratory has been the synthesis and structural characterization of transition metal–boron hybrid clusters, and a number of such species have been obtained from the treatment of $B_5H_8^-$ ion with metal ions in the presence of $C_5H_5^-$ in tetrahydrofuran (THF). With $CoCl_2$[4,5] the main isolable product was the monocobalt complex 2-$(\eta^5\text{-}C_5H_5)CoB_4H_8$, which was further metalated to give the first known closo metalloboranes including $(\eta^5\text{-}C_5H_5)_2Co_2B_4H_6$, $(\eta^5\text{-}C_5H_5)_3Co_3B_3H_5$, $(\eta^5\text{-}C_5H_5)_3Co_3B_4H_4$, and $(\eta^5\text{-}C_5H_5)_4Co_4B_4H_4$; our earlier structural assignments[4,5] for these molecules have been confirmed crystallographically.[6] With $FeCl_2$,[7] only monometallic products have been isolated from the $B_5H_8^-$ reaction, notably 2-$(\eta^5\text{-}C_5H_5)FeB_5H_{10}$ (a ferrocene analogue) and $(\eta^5\text{-}C_5H_5)FeB_{10}H_{15}$. With $NiBr_2$ the products did not correspond to those obtained in either the iron or cobalt systems, and the nickelocene–$B_5H_8^-$ reaction in the presence of sodium amalgam gave still different results.

The cobalt and iron systems have been fully described elsewhere,[4,5,7] and a preliminary communication on the nickelocene–$B_5H_8^-$ reaction has appeared.[8] In this article we present a detailed account of several reactions involving nickel insertion into the $B_5H_8^-$ and $(CH_3)_2C_2B_4H_5^-$ ions, including the structural characterization of the nickelaborane and nickelacarborane products.

Results and Discussion

Preparation of *closo*-1,7-$(\eta^5\text{-}C_5H_5)_2Ni_2B_{10}H_{10}$ and *closo*-1,6-$(\eta^5\text{-}C_5H_5)_2Ni_2B_8H_8$ from B_5H_8, $NiBr_2$, and $C_5H_5^-$. Our initial attempts to effect nickel insertion into the $B_5H_8^-$ ion utilized nickel bromide and sodium cyclopentadienide in THF solution at room temperature, from which two dinickel closo boranes were isolated in low yield by column chromatography along with traces of other products.

$$\begin{array}{l} B_5H_8^- + Ni^{2+} + C_5H_5^- \rightarrow \\ \qquad \underset{\text{yellow (I)}}{(\eta^5\text{-}C_5H_5)_2Ni_2B_{10}H_{10}} + \underset{\text{orange (II)}}{(\eta^5\text{-}C_5H_5)_2Ni_2B_8H_8} \\ \qquad\qquad + \underset{\text{brown (trace, III)}}{(\eta^5\text{-}C_5H_5)_2Ni_2B_{10}H_{10}} \end{array}$$

The yellow product I is an isomer of a brown compound, $(\eta^5\text{-}C_5H_5)_2Ni_2B_{10}H_{10}$, recently obtained by Hawthorne et al. from the reaction of nickelocene and $B_{10}H_{10}^{2-}$ ion.[9] The ^{11}B and ^1H NMR spectra of I (Tables I and II) indicate mirror or twofold symmetry and are consistent with a closo 12-vertex (icosahedral) structure analogous to $C_2B_{10}H_{12}$, but do not

0002-7863/79/1501-6229$01.00/0

Table I. 32.1-MHz ^{11}B FT NMR Data ($CDCl_3$ Solution)

compd	σ, ppm[a] (*J*, Hz)	rel area
1,7-$(C_5H_5)_2Ni_2B_{10}H_{10}$ (I)	38.9 (149), 20.3 (149), −3.9 (151)	4:4:2
1,6-$(C_5H_5)_2Ni_2B_8H_8$ (II)	93.6 (145), 47.5 (147), 20.4 (145), 12.2 (140), 6.7 (137)	1:2:2:1:2
$(C_5H_5)_4Ni_4B_4H_4$ (IV)	56.2 (156)	
$(C_5H_5)_4Ni_4B_5H_5$ (V)	64.7 (156), 55.0 (157), 29.4 (117)	2:1:2
$(C_5H_5)_2Ni_2(CH_3)_2C_2B_4H_4$ (VI)	24.6 (166), 3.2 (156)	2:2
$(C_5H_5)_2Ni_2(CH_3)_2C_2B_5H_5$ (VII)	30.1 (146), 1.2 (156), −2.8 (127)	1:2:2

[a] Parts per million relative to $BF_3{\cdot}O(C_2H_5)_2$ with positive sign indicating shift to lower field (less shielding).

Table II. 100-MHz ^1H FT NMR Data ($CDCl_3$ Solution)

compd	ppm (rel area)[a]	assignment
I	5.27	C_5H_5
II	5.82 (5), 5.40 (5)	C_5H_5
IV	5.34 (5)	C_5H_5
	8.22 (1)[b]	H-B
V	5.45 (5), 5.35 (10), 5.29 (5)	C_5H_5
	8.80 (2),[b] 7.25 (1),[b] 4.70 (2)[b]	H-B
VI	5.25 (5)	C_5H_5
	1.91 (3)	CH_3
VII	5.26 (10)	C_5H_5
	2.06 (3), 1.85 (3)	CH_3

[a] Parts per million relative to $(CH_3)_4Si$ with positive sign indicating shift to lower field. [b] H-B singlet observed on ^{11}B decoupling.

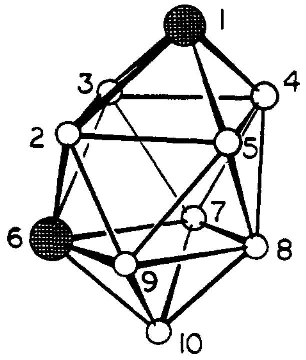

Figure 1. Proposed structure of 1,6-$(\eta^5\text{-}C_5H_5)_2Ni_2B_8H_8$ (II). Shaded circles represent $Ni(\eta^5\text{-}C_5H_5)$.

Table III. Infrared Absorptions (CCl_4 Solution vs. CCl_4, cm^{-1})

I[a]	2960 (m), 2935 (s), 2860 (m, sh), 2525 (m), 1725 (m), 1465 (m, br), 1280 (s, br), 1260 (m), 1140 (w), 1125 (w), 1075 (w), 825 (w)
II[a]	2950 (sh), 2920 (s), 2850 (m), 2580 (w), 2510 (s), 1730 (m, br), 1580 (m, br), 1540 (m), 1460 (m), 915 (w)
IV	2950 (sh), 2920 (s), 2850 (m), 2445 (s), 1410 (m), 1340 (m), 1210 (m), 1115 (w), 1050 (m), 1005 (m), 900 (w)
V	2950 (sh), 2920 (s), 2850 (m), 2470 (s), 2440 (s, sh), 1710 (w, br), 1460 (w), 1410 (w), 1340 (m), 1260 (m), 1100 (w), 1005 (m), 905 (w), 770 (m)
VI	2940 (m), 2910 (vs), 2850 (s), 2530 (vs), 2500 (vs), 1780 (w), 1600 (w, br), 1440 (m), 1410 (w), 1360 (w), 1330 (w), 1240 (w, br), 1105 (m), 1045 (w), 1005 (m-s), 940 (m), 910 (w), 865 (m), 840 (w)
VII	3045 (m), 2950 (sh, s), 910 (vvs), 2880 (s), 2720 (w), 2560 (sh, s), 2530 (vvs), 1790 (w), 1705 (s, br), 1610 (s, br), 1440 (vs), 1380 (vs, br), 1340 (m, br), 1290 (sh), 1260 (w, sh), 1040 (w, sh), 1005 (s, br), 995 (sh), 955 (s), 895 (s), 845 (w)

[a] CH_2Cl_2 solution vs. CH_2Cl_2.

Table IV. Electronic Spectra, CH_2Cl_2 Solution

compd	λ_{max}, nm (log ε)
$(\eta^5\text{-}C_5H_5)_4Ni_4B_4H_4$ (IV)	543 (4.54), 423 sh (4.43), 335 (4.69), 284 (4.72)
$(\eta^5\text{-}C_5H_5)_4Ni_4B_5H_5$ (V)	548 (2.84), ~365 sh (3.99), 302 sh (4.35), 257 (4.45)

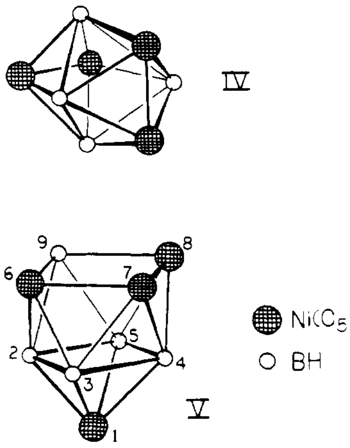

Figure 2. Established cage structures of $(\eta^5\text{-}C_5H_5)_4Ni_4B_4H_4$ (IV) and $(\eta^5\text{-}C_5H_5)_4Ni_4B_5H_5$ (V).

allow an unequivocal choice between 1,2 (ortho) and 1,7 (meta) arrangements of the nickel atoms. However, the brown isomer of $(\eta^5\text{-}C_5H_5)_2Ni_2B_{10}H_{10}$ (apparently identical with III) has been tentatively assigned the 1,2 structure,[9c] in which case I is the 1,7; in addition, the fact that the nickel atoms adopt nonadjacent vertices in compound II (vide infra) indicates at least that mechanisms for nonvicinal metal insertion are operative in this reaction. (This observation contrasts with other reaction systems to be described below.)

Compound II is a ten-vertex Ni_2B_8 system which is cage isoelectronic with *closo*-$C_2B_8H_{10}$ (since $(\eta^5\text{-}C_5H_5)Ni$ and CH are both formal three-electron donors to skeletal bonding[3a]), and the structure in Figure 1 is proposed from NMR data. Assuming normal ten-vertex closo geometry (bicapped square antiprism), there is a mirror plane on which are located two nonequivalent nickel atoms and two unique borons; the metals must then occupy either the 1,2 or 1,6 vertices. However, the observation of a very low field ^{11}B shift for one of the boron nuclei indicates the presence of a low-coordinate boron adjacent to a metal atom,[10] thus favoring the 1,6 structure.

These results differ sharply from the corresponding reaction of $CoCl_2$ and NaC_5H_5 with $B_5H_8^-$ ion,[4] which as already noted generates clusters containing up to four metal atoms, and which produces no species analogous to I-III. Since only dimetallic complexes were obtained in the $NiBr_2$ reaction, and the yields of these were low, it appeared worthwhile to utilize nickelocene/sodium amalgam[9c] as the metal reagent in place of $NiBr_2$ and $C_5H_5^-$.

Preparation of $(\eta^5\text{-}C_5H_5)_4Ni_4B_4H_4$ and $(\eta^5\text{-}C_5H_5)_4Ni_4B_5H_5$ from $B_5H_8^-$ Ion and Nickelocene. In the presence of 1 molar equiv of sodium amalgam, the sodium salt of $B_5H_8^-$ reacts readily with nickelocene in cold THF (when only catalytic amounts of sodium are employed the reaction rate is extremely slow, and in the absence of sodium there is little, if any, reaction). Two air-stable nickel-boron clusters have been isolated in highly variable yield, purified with the aid of preparative-

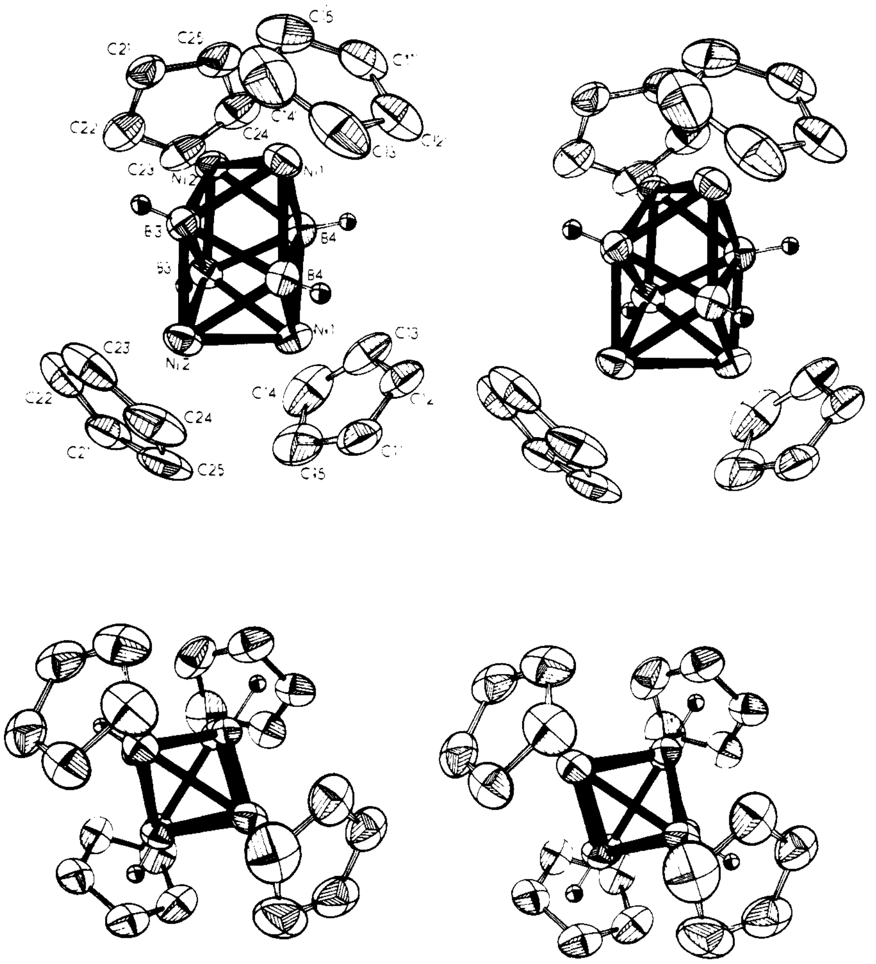

Figure 3. Stereoviews of the molecular structure of $(\eta^5\text{-}C_5H_5)_4Ni_4B_4H_4$. Thermal ellipsoids enclose 50% of the electron density, except for cage hydrogen atoms, which are drawn with arbitrary radius.

scale high-pressure liquid chromatography, and characterized as brown $(\eta^5\text{-}C_5H_5)_4Ni_4B_4H_4$ (IV) and green $(\eta^5\text{-}C_5H_5)_4Ni_4B_5H_5$ (V); in addition, compound II was isolated, and compound I and a probable $(\eta^5\text{-}C_5H_5)_3Ni_3B_7H_8$ have been found in very low yields. The principal product of the reaction is an intractable dark solid, which is essentially insoluble in organic solvents and is vigorously reactive with water.

The metal-rich clusters IV and V are only the second and third examples of metalloboron cages containing four metal atoms (the first being $(\eta^5\text{-}C_5H_5)_4Co_4B_4H_4$[4,5]), and were characterized by ^{11}B and ^1H FT NMR spectroscopy (Tables I and II), infrared (Table III), UV-visible spectroscopy (Table IV), unit- and high-resolution mass spectroscopy (Experimental Section), and an X-ray diffraction study of IV.

Structure of $(\eta^5\text{-}C_5H_5)_4Ni_4B_4H_4$ (IV). The ^{11}B and ^1H FT NMR spectra of IV surprisingly revealed single boron and nickel environments, indicating either a static structure of high symmetry or a fluxional molecule. A closo D_{2d} structure analogous to that previously established[6c] for $(\eta^5\text{-}C_5H_5)_4Co_4B_4H_4$ is consistent with the NMR data but violates the electron-counting rules[3a] for clusters: since the $Ni(C_5H_5)$ and BH units contribute respectively three and two electrons to framework bonding, the cage is an 8-vertex, 20-electron ($2n + 4$) system and would be expected to adopt a nido (open-cage) shape. However, an X-ray crystallographic analysis of IV confirmed the closo structure in Figure 2, in which the four nickel atoms adopt low-coordinate vertices on the "ends" of the cage. Tables V–VIII contain data relevant to the crystal structure determination, and two stereoviews of the molecule are presented in Figure 3.

The complex is bisected by a crystallographic twofold axis passing through the midpoints of the B(3)–B(3′) and B(4)–B(4′) bonds, and the Ni_4B_4 cage has nearly D_{2d} symmetry. This is apparent from the fact that the groups Ni(1)–Ni(2)–B(3′)–B(4′) and Ni(1′)–Ni(2′)–B(3)–B(4) are each nearly planar (Table VIII) and intersect at an angle of 90° within experimental error. It is also noteworthy that the four Ni–B–Ni–B diamond-shaped sides of the polyhedron are planar (Table VIII, planes 5, 6, 7, and 8) and are mutually perpendicular. The cage is unquestionably closo, with no evidence of distortion toward either nido or capped-closo geometry.

A particularly significant question in this complex concerns the nature of the metal–metal interaction, which has several unusual aspects. The fact that the nickel atoms adopt the low-coordinate vertices on the D_{2d} polyhedron is in contrast to the cobalt species $(\eta^5\text{-}C_5H_5)_4Co_4B_4H_4$, where the cobalts occupy the high-coordinate positions and form a contiguous belt around the middle of the cage;[6c] thus, in the cobalt complex there are four metal–metal links, and in the nickel species only two. In addition, there are several indications that the Ni–Ni interactions in IV involve strong localized bonds: (1) The equivalent Ni–Ni distances of 2.354 (1) Å are the shortest metal–metal vectors yet observed in a metalloborane or metallocarborane;[11] shorter Ni–Ni distances (down to 2.33 Å) have to our knowledge been found only in a few clusters in which the metals are bridged by carbonyl or alkyne groups.[13] Indeed, Ruff, White, and Dahl[13b] cite 2.34 Å as the approximate distance corresponding to a Ni–Ni single bond. (2) The mean bonded B–B distance in IV (1.928 Å) is unusually long. (3) The mean $Ni\text{-}C_5H_5$ distance (normal to the ring plane)

Table V. Positional and Thermal Parameters and Their Estimated Standard Deviations for $(C_5H_5)_4Ni_4B_4H_4$[a]

atom	X	Y	Z	B_{11}	B_{22}	B_{33}	B_{12}	B_{13}	B_{23}
Ni(1)	0.076 44(3)	0.082 21(9)	−0.148 16(4)	2.73(2)	3.55(3)	2.79(2)	0.73(2)	0.59(2)	−0.20(2)
Ni(2)	0.090 84(3)	0.298 76(9)	−0.255 76(5)	2.11(2)	3.31(3)	3.74(3)	−0.34(2)	1.18(2)	−0.62(2)
C(11)	0.1684(3)	−0.0879(9)	−0.1020(5)	3.5(2)	5.3(3)	5.3(3)	1.3(2)	0.6(2)	1.1(3)
C(12)	0.1083(3)	−0.1763(9)	−0.0888(4)	4.0(2)	5.3(3)	4.7(2)	1.7(2)	1.5(2)	1.7(2)
C(13)	0.0808(4)	−0.0746(10)	−0.0281(4)	6.0(3)	7.1(4)	3.9(2)	3.1(3)	1.3(2)	1.6(3)
C(14)	0.1230(5)	0.0778(11)	−0.0008(4)	9.3(5)	7.2(4)	3.0(2)	3.1(4)	−0.3(3)	−0.5(3)
C(15)	0.1802(4)	0.0736(10)	−0.0510(5)	5.2(3)	7.0(4)	5.3(3)	0.7(3)	−2.2(3)	0.3(3)
C(21)	0.1807(3)	0.4720(8)	−0.1983(4)	2.7(2)	4.6(3)	5.5(3)	−1.1(2)	1.3(2)	−1.3(2)
C(22)	0.1313(3)	0.5530(9)	−0.2763(5)	4.2(2)	4.6(3)	5.6(3)	−1.9(2)	1.9(2)	0.1(2)
C(23)	0.1254(3)	0.4375(9)	−0.3574(4)	4.0(2)	6.6(3)	4.7(2)	−2.6(2)	2.1(2)	−0.5(3)
C(24)	0.1710(3)	0.2914(10)	−0.3293(5)	3.2(2)	7.3(4)	6.2(3)	−1.6(3)	2.8(2)	−1.8(3)
C(25)	0.2051(3)	0.3089(9)	−0.2316(5)	2.1(2)	6.2(3)	7.9(3)	−1.3(2)	2.1(2)	−1.7(3)
B(3)	0.0160(3)	0.3067(8)	−0.1821(4)	2.7(2)	2.9(2)	3.0(2)	−0.1(2)	1.2(2)	−0.7(2)
B(4)	0.0298(3)	0.0739(8)	−0.2891(4)	3.2(2)	2.7(2)	2.3(2)	0.1(2)	0.9(2)	−0.0(2)
H(3)[b]	0.026(2)	0.383(7)	−0.134(3)	3.(1)					
H(4)	0.047(2)	−0.027(6)	−0.332(3)	3.(1)					

[a] The form of the anisotropic thermal parameter is $\exp[-B_{11}h^2(a^*)^2 + B_{22}k^2(b^*)^2 + B_{33}l^2(c^*)^2)/4 + (B_{12}hka^*b^* + B_{13}hla^*c^* + B_{23}klb^*c^*)/2]$. [b] For all hydrogen atoms, standard isotropic B values are reported.

Table VI. Interatomic Distances (Å)[a] in $(\eta^5\text{-}C_5H_5)_4Ni_4B_4H_4$

Ni(1)-Ni(1′)	3.591(1)	Ni(2)-C(24)	2.153(4)
Ni(1)-Ni(2)	2.354(1)	Ni(2)-C(25)	2.160(3)
Ni(1)-Ni(2′)	3.563(1)	B(3)-B(3′)	1.932(7)
Ni(1)-B(3)	2.037(4)	B(3)-B(4′)	1.955(5)
Ni(1)-B(4)	2.031(3)	B(3)-H(3)	0.89(3)
Ni(1)-B(4)	2.018(4)	B(4)-B(4′)	1.868(7)
Ni(1)-C(11)	2.151(4)	B(4)-H(4)	1.10(3)
Ni(1)-C(12)	2.150(4)	C(11)-C(12)	1.411(5)
Ni(1)-C(13)	2.119(4)	C(12)-C(13)	1.402(6)
Ni(1)-C(14)	2.116(4)	C(13)-C(14)	1.401(7)
Ni(1)-C(15)	2.126(4)	C(14)-C(15)	1.513(7)
Ni(2)-Ni(2′)	3.604(1)	C(15)-C(11)	1.414(6)
Ni(2)-B(3)	2.063(4)	C(21)-C(22)	1.415(6)
Ni(2)-B(3′)	2.028(4)	C(22)-C(23)	1.462(6)
Ni(2)-B(4)	2.045(4)	C(23)-C(24)	1.400(6)
Ni(2)-C(21)	2.155(3)	C(24)-C(25)	1.419(6)
Ni(2)-C(22)	2.123(4)	C(25)-C(21)	1.452(5)
Ni(2)-C(23)	2.100(4)		

[a] Primed atoms are related to their unprimed counterparts by the twofold rotation axis at $z = -0.25$.

Table VII. Selected Bond Angles (deg) in $(\eta^5\text{-}C_5H_5)_4Ni_4B_4H_4$

Ni(2)-Ni(1)-B(3)	55.5(1)	Ni(1)-B(4)-H(4)	120(2)
Ni(2)-Ni(1)-B(4)	55.0(1)	Ni(2)-B(4)-H(4)	117(2)
B(3)-Ni(1)-B(4′)	57.6(1)	B(3′)-B(4)-H(4)	133(2)
B(4)-Ni(1)-B(4′)	54.9(2)	B(4′)-B(4)-H(4)	135(2)
Ni(1)-Ni(2)-B(3)	54.4(1)	Ni(2)-B(3′)-B(3)	62.8(2)
Ni(1)-Ni(2)-B(4)	54.5(1)	Ni(2)-B(3′)-B(4)	61.8(2)
B(3)-Ni(2)-B(3′)	56.4(2)	Ni(1)-B(4′)-B(3)	61.7(2)
B(4)-Ni(2)-B(3′)	57.4(1)	Ni(1)-B(4′)-B(4)	62.9(3)
Ni(1)-B(3)-Ni(2)	70.1(1)	C(12)-C(11)-C(15)	110.1(4)
Ni(1)-B(3)-B(4′)	60.7(2)	C(11)-C(12)-C(13)	108.8(4)
Ni(2)-B(3)-B(3′)	60.9(2)	C(12)-C(13)-C(14)	109.2(4)
Ni(1)-B(3)-H(3)	111(2)	C(13)-C(14)-C(15)	107.3(4)
Ni(2)-B(3)-H(3)	115(2)	C(14)-C(15)-C(11)	104.6(4)
B(3′)-B(3)-H(3)	140(2)	C(22)-C(21)-C(25)	107.3(4)
B(4′)-B(3)-H(3)	137(2)	C(21)-C(22)-C(23)	107.0(4)
Ni(1)-B(4)-Ni(2)	70.6(1)	C(22)-C(23)-C(24)	109.1(4)
Ni(1)-B(4)-B(4′)	62.2(2)	C(23)-C(24)-C(25)	107.7(4)
Ni(2)-B(4)-B(3′)	60.9(2)	C(24)-C(25)-C(21)	108.9(4)

is a rather long 1.755 Å. These observations are consistent with a concentration of electron density in the Ni-Ni vectors at the expense of other regions of the molecule.

Further discussion of the structure of IV will be given in the concluding section.

Structure of $(\eta^5\text{-}C_5H_5)_4Ni_4B_5H_5$ (V). The skeletal electron count[3] in V is 22, corresponding to a $(2n + 4)$-electron cage which was expected[8] to adopt a nine-vertex nido structure, most likely a monocapped square antiprism. This prediction has been borne out by an X-ray crystallographic study of V,[14] which, however, revealed that the $(C_5H_5)Ni$ groups occupy vertices 1, 6, 7, and 8 (Figure 2) instead of 1, 2, 7, and 8 as we originally proposed.[8] Both arrangements are consistent with ^{11}B and ^1H NMR spectra, but it is interesting that the known structure of V corresponds to that of the known metallocarborane $(\eta^5\text{-}C_5H_5)Ni_3CB_5H_6$,[15] in which the nickel atoms occupy the 6, 7, and 8 vertices while the CH unit is in the apex (1) position.

Chemical Properties of $(\eta^5\text{-}C_5H_5)_4Ni_4B_4H_4$ (IV) and $(\eta^5\text{-}C_5H_5)_4Ni_4B_5H_5$ (V). Treatment of V with KOH in ethanol at room temperature for 12 h resulted in partial decomposition to uncharacterizable products, but half of the original sample of V was recovered. The only identifiable product was IV, obtained in 12% yield. The fact that IV can be generated from V implies that the IV obtained in the nickelocene–$B_5H_8^-$ reaction is formed directly from V, probably by abstraction of BH by a reactive fragment such as $C_5H_5^-$. (One possible mechanism involves removal of B(2)–H from V followed by movement of Ni(6) into the 2 position, with subsequent closure of the polyhedron to give IV.) The overall sequence of events would then consist of insertion of four $(C_5H_5)Ni^{n+}$ units into the pentaborane anion with loss of hydrogen to give V, followed by partial degradation of V to IV.

On heating for several hours at 140 °C, both IV and V partially decomposed to black solids, and both compounds degraded slowly on treatment with HCl in THF. The detailed chemistry of these tetranickel complexes is under study and will be reported in due course.

Preparation of Dinickel Metallocarboranes from $(CH_3)_2C_2B_4H_5^-$ Ion and Nickelocene. In light of the syntheses of IV and V from $B_5H_8^-$ and nickelocene it appeared likely that incorporation of $(C_5H_5)Ni^{n+}$ into the nido-carborane substrate $C_2B_4H_7^-$ or its *C,C′*-dimethyl derivative could be achieved since these carborane anions have been shown to be highly amenable to transition-metal insertion.[1,16] Accordingly, a solution of $Na^+(CH_3)_2C_2B_4H_5^-$ in THF (prepared[17] from *nido*-$(CH_3)_2C_2B_4H_6$ and NaH) was added to a nickelocene–sodium amalgam mixture at −78 °C. Following reaction at room temperature for 12 h and workup in air, TLC separation gave a series of products which were isolated in low yields and

Table VIII. Selected Mean Planes

atom	deviation	atom	deviation
Plane 1: Ni(2), B(3), B(4), B(4′) $-0.4840x + 0.4504y - 0.7503z = 2.4035$			
Ni(2)	−0.050	B(4′)	−0.056
B(3)	0.051	Ni(1)	−1.573
B(4)	0.055		
Plane 2: Ni(1), B(3), B(4), B(3′) $0.8902x + 0.4469y - 0.0891z = 2.2957$			
Ni(1)	0.061	B(3′)	0.066
B(3)	−0.064	Ni(2)	1.584
B(4)	−0.063		
Plane 3: Ni(1), Ni(2), B(3′), B(4′) $0.3106x - 0.7083y - 0.6339z = 1.5845$			
Ni(1)	−0.024	Ni(1′)	1.155
Ni(2)	0.024	Ni(2′)	−1.198
B(3′)	−0.024	B(3)	−1.234
B(4′)	0.024	B(4)	1.195
Plane 4: Ni(1′), N(2′), B(3), B(4) $0.3106x + 0.7083y - 0.6339z = 3.5903$			
Plane 5: Ni(1), Ni(1′), B(4), B(4′) $y = 0.5856$			
Ni(1)	−0.031	Ni(2)	−1.658
Ni(1′)	−0.031	Ni(2′)	−1.658
B(4)	0.031	B(3)	−1.717
B(4′)	0.031	B(3′)	−1.717
Plane 6: Ni(2), Ni(2′), B(3), B(3′) $y = 2.2746$			
Ni(2)	−0.030	Ni(1)	−1.656
Ni(2′)	−0.030	Ni(1′)	−1.656
B(3)	0.030	B(4)	−1.718
B(3′)	0.030	B(4′)	−1.719
Plane 7: Ni(1), Ni(2′), B(3), B(4′) $0.4388x + 0.0160y - 0.8984z = 2.8412$			
Ni(1)	−0.004	Ni(1′)	1.672
Ni(2′)	−0.004	Ni(2)	1.724
B(3)	0.004	B(3′)	1.718
B(4′)	0.004	B(4)	1.662
Plane 8: Ni(1′), Ni(2), B(3′), B(4) $0.4388x - 0.0160y - 0.8984z = 4.4895$			
Plane 9: C(11), C(12), C(13), C(14), C(15) $0.3819x - 0.4878y + 0.7814z = 0.6305$			
C(11)	−0.008	C(14)	−0.012
C(12)	0.000	C(15)	0.012
C(13)	0.008	Ni(1)	1.752
Plane 10: C(21), C(22), C(23), C(24), C(25) $0.8385x + 0.5052y - 0.2043z = 6.0397$			
C(21)	0.000	C(24)	0.005
C(22)	0.004	C(25)	−0.003
C(23)	−0.006	Ni(2)	−1.758

planes	angle	planes	angle
1,9	6.1	4,7	44.2
2,10	8.0	4,8	46.0
3,4	89.8	5,6	0.0
3,5	44.9	5,7	89.1
3,6	44.9	5,8	89.1
3,7	46.0	6,7	89.1
3,8	44.2	6,8	89.1
4,5	44.9	7,8	1.8
4,6	44.9	9,10	85.4

characterized as green $(\eta^5\text{-}C_5H_5)_2Ni_2(CH_3)_2C_2B_4H_4$ (VI), brown $(\eta^5\text{-}C_5H_5)_2Ni_2(CH_3)_2C_2B_5H_5$ (VII), and apparent $\sigma\text{-}C_5H_7$- and $\sigma\text{-}C_5H_9$-substituted derivatives of VI and VII.

The structural characterization of VI poses interesting questions which relate to the established structure of IV, discussed above, and to electron-counting considerations. Since $Ni(C_5H_5)$ and CH are formally equivalent in terms of skeletal electron contributions,[3a] the $Ni_2C_2B_4$ species, VI, is an isoelectronic analogue of the Ni_4B_4 complex, IV. Consequently, one might expect VI to adopt a closo structure analogous to IV, as shown in Figure 4, despite the fact that this violates the prediction of nido geometry for this 20-electron $(2n + 4)$ system. The closo structure depicted is consistent with the ^{11}B and ^1H FT NMR spectra, which indicate high symmetry on the NMR time scale; it is further supported by the strong probability that the framework carbon atoms remain adjacent (as they are in the carborane substrate) and that the nickel atoms adopt low-coordinate vertices, as they have a tendency to do when possible in nickel-boron clusters.[8,9c,15] We shall have more to say about VI below.

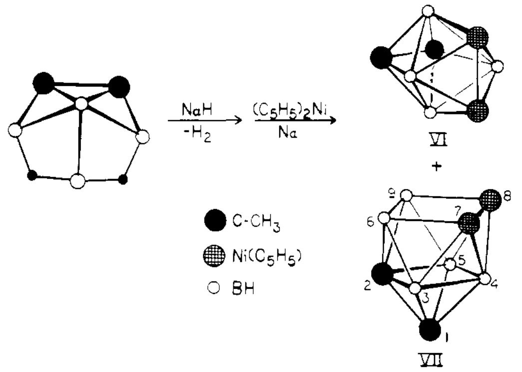

Figure 4. Reaction scheme for the synthesis of $(\eta^5\text{-}C_5H_5)_2Ni_2(CH_3)_2C_2B_4H_4$ (VI) and $(\eta^5\text{-}C_5H_5)_2Ni_2(CH_3)_2C_2B_5H_5$ (VII) from $2,3\text{-}(CH_3)_2C_2B_4H_6$, showing proposed structures of the products.

Compound VII is formulated as a nine-vertex nido species, electronically analogous to $(\eta^5\text{-}C_5H_5)_4Ni_4B_5H_5$ (V). The ^{11}B and ^1H NMR data indicate mirror symmetry with equivalent $Ni(C_5H_5)$ units, nonequivalent $C\text{-}CH_3$ groups, and a 1:2:2 pattern of BH resonances. Assuming a monocapped square antiprism (the geometry established for the analogous clusters V[14] and $(\eta^5\text{-}C_5H_5)_3Ni_3CB_5H_6$[15]), the cage carbon atoms and the unique boron are on a mirror plane. The nickel atoms then occupy the (3,5), (6,9), or (7,8) vertices, but the 7,8 arrangement (Figure 4) is preferred since it permits straightforward conversion to VI by removal of B(6) or B(9) with subsequent cage closure. All three structures have low-coordinate boron atoms adjacent to nickel, and it is surprising that the expected low-field ^{11}B NMR signals normally associated with such borons do not appear (the resonance at δ +30 must be assigned to the unique high-coordinate B(4) in any case). We note, however, that the low-coordinate B(6) and B(9) atoms in the proposed structure are each adjacent to only one metal, and the low-field shift is usually less pronounced in such situations compared to those in which boron is coordinated to two or three metal atoms. Nevertheless, this structure remains in some doubt, and an X-ray study is planned.

Summary

Mechanistic Aspects. In many of the metalloborane syntheses reported to date, yields of the isolated products have been low, largely owing to the formation of insoluble or intractable polymeric material; this is particularly true of the reactions of $B_5H_8^-$ ion with iron, cobalt, and nickel reagents.[4,5,7,8] In such cases the isolated monomeric products necessarily reflect only a part of the overall reaction chemistry, but a most important part nonetheless. With respect to the *isolable metalloborane products*, on which our research has centered, the present results can be compared in some interesting ways with earlier studies of metalloboranes in our own as well as other laboratories.

1. The reactions of $FeCl_2$, $CoCl_2$, and $NiBr_2$ with $B_5H_8^-$ and $C_5H_5^-$ in THF proceed so differently that the types of isolated metalloboranes obtained are mutually exclusive: $FeCl_2$ yields only monometallic species,[7] $CoCl_2$ gives one-, two-, three-, and four-metal clusters,[4,5] and $NiBr_2$ generates dimetallic systems, with no instance in which structural analogues are obtained from different metals. The isolated products are of considerable structural interest but the mechanistic processes involved in their syntheses are obscure.

2. In reactions of metallocenes and sodium amalgam with $B_5H_8^-$ in THF, the metalloborane products contain even numbers of metal atoms, with $M(\eta^5\text{-}C_5H_5)$ groups adopting adjacent locations in the cage framework. Thus, the main metalloborane products of the interaction with $Co(C_5H_5)_2$[18] are $(C_5H_5)_2Co_2B_4H_6$ and $(C_5H_5)_4Co_4B_4H_4$ (both identical with products of the $CoCl_2/C_5H_5^-$ reaction[4,5]), and $Ni(C_5H_5)_2$ produces tetrametallic species as described above. The tendency for successive addition of $M(\eta^5\text{-}C_5H_5)$ units to occur in adjacent vertices is also observed in the reactions of nickelocene with $B_{10}H_{10}^{2-}$ ion[9c] and with CB_5H_9,[15] which produce di- and trinickel species, respectively. In addition, metallocarborane chemistry is replete with examples of the insertion of second (or subsequent) metal atoms into a monometallic carborane cage at locations adjacent to the first metal;[19] in most cases metal-cyclopentadienyl groups are involved, but $M(CO)_3$ units also exhibit this effect. The clear implication of this evidence is that the first metal atom to be incorporated into the cage exerts a directive influence on the entry of additional metals, frequently in such a way as to promote metal-metal binding. This effect is surely electronic, and overrides the steric inhibition of adjacent incorporation of metals that one would expect from the bulky C_5H_5 ligands. These two opposing tendencies—electronic favoring of metal-metal binding and steric hindrance which discourages it—are of roughly comparable importance, and the result can go either way depending on the specific system involved. In the nine-vertex *closo*-cobaltacarborane $(\eta^5\text{-}C_5H_5)_2Co_2C_2B_5H_7$ there is a delicate balance between the two effects,[19c,m] such that isomers with adjacent and nonadjacent cobalt atoms exist in equilibrium in the vapor phase ($K_{eq} = 1.00$ at 340 °C).

3. There is a sharp contrast between the reactions of metal reagents with $B_5H_8^-$ ion and with larger anions such as $B_{11}H_{13}^{2-}$, $B_{10}H_{13}^-$, $B_9H_{12}^-$, and $B_nH_n^{2-}$ (n = 9, 10, 11). With the large ions,[9c] metal insertions tend to proceed with little or no cage degradation to give products that are direct structural extensions of the original borane. The more reactive $B_5H_8^-$ ion, however, generates structurally diverse products which reflect complex reaction mechanisms (a remarkable example of this is the absence of a single five-boron species among the many isolable products of the $B_5H_8^-$-$CoCl_2$-$C_5H_5^-$ reaction[4,5]). In addition, it will be noted that tetrametallic species have thus far been obtained only from $B_5H_8^-$; the large borane anions readily accept one or two $Ni(C_5H_5)$ units[9c] but further metalation has not been observed. We have no explanation for this at present.

Structural Aspects. The eight-vertex clusters $(\eta^5\text{-}C_5H_5)_4Ni_4B_4H_4$ (IV) and $(\eta^5\text{-}C_5H_5)_2Ni_2(CH_3)_2C_2B_4H_4$ (VI) require further comment. The observation of D_{2d} closo geometry for IV, and the assignment of the same structure to VI from NMR data, is in line with the pattern generally observed in eight-vertex clusters. As we have noted elsewhere,[6c] all of the structurally characterized eight-vertex boron and heteroboron cages (except for those with bridging hydrogen atoms) are known to have D_{2d} closo structures. It is striking that this geometry is found not only for $B_8H_8^{2-}$[20] and $(CH_3)_2C_2B_6H_6$,[21] with 18 skeletal electrons, but also for $(\eta^5\text{-}C_5H_5)_4Co_4B_4H_4$[6c] and B_8Cl_8,[22] with 16, and for $(\eta^5\text{-}C_5H_5)_4Ni_4B_4H_4$, with 20. The 16- and 20-electron species constitute violations of Wade's rules, and we have suggested[6c] that their apparent failure for eight-vertex polyhedra may be traced to special geometric qualities of the D_{2d} dodecahedron, including high symmetry and high average vertex coordination number (in comparison to alternative eight-vertex geometries). Thus, while several cage structures may be energetically accessible for eight-vertex boron polyhedra (as is apparently the case[23] for $B_8H_8^{2-}$), *in the solid state* there is a distinct preference for closo geometry regardless of the framework electron count; however, the possibility of fluxionality *in solution*, involving geometries other than D_{2d} closo, cannot be excluded.

The dinickel metallocarborane $(\eta^5\text{-}C_5H_5)_2Ni_2(CH_3)_2C_2B_4H_4$ (VI) as noted earlier is analogous to the tetranickel cluster IV, and its NMR spectra support a similar D_{2d} closo structure with the heteroatoms in low-coordinate vertices; thus, formal replacement of two $Ni(C_5H_5)$ by two electronically equivalent CH units does not appear to alter the basic cage geometry. On this basis one would expect $(CH_3)_4C_4B_4H_4$ to adopt an analogous structure, but a carborane of this composition prepared by Fehlner[24] apparently does not; its ^{11}B and ^1H NMR spectra are incompatible with a static D_{2d} cage. Obviously, additional crystal structure determinations in this area are required.

In this and earlier discussions[6c] of eight-vertex polyhedra we have assumed that the compounds described represent thermodynamically favored cage structures. However, it is important to consider whether the observed structures of $(\eta^5\text{-}C_5H_5)_4Ni_4B_4H_4$, $(\eta^5\text{-}C_5H_5)Co_4B_4H_4$, and related compounds might in fact be kinetically rather than thermodynamically stabilized arrangements. In the metallocarborane area there are many examples of kinetic stabilization of complexes which require high activation energy for rearrangement,[25] and are constrained, except at high temperatures, to unfavorable (even bizarre) cage geometries [e.g., the 14-vertex $(\eta^5\text{-}C_5H_5)_2Fe_2(CH_3)_4C_4B_8H_8$ isomers[25e]]. In our view it is highly unlikely that this is the case with the eight-vertex species in general, since low-energy rearrangement mechanisms[23c] exist for $B_8H_8^{2-}$ and are likely for other eight-vertex systems as well. It seems significant that the eight-vertex systems $(\eta^5\text{-}C_5H_5)CoC_2B_5H_7$ and $(\eta^5\text{-}C_5H_5)_2Co_2C_2B_4H_6$ have each been obtained in only one isomeric form and do not undergo thermal rearrangement,[25d] whereas 7-, 9-, 10-, 11-, 12-, and 13-vertex cobaltacarboranes occur as isomers and *do* rearrange.[25a-d] Moreover, the high symmetry of the Ni_4B_4 and Co_4B_4 clusters, and the fact that only one isomer of each is obtained,[26] supports the view that the observed structures are in fact the preferred arrangements for these systems.

There is a possibility that the proposed geometry of $(\eta^5\text{-}C_5H_5)_2Ni_2(CH_3)_2C_2B_4H_4$ (Figure 4) may not be the most stable form for that system, if the normal tendency of framework carbon atoms to achieve mutual separation is operative here, but this could be counterbalanced by the preference of carbon (and nickel) for low-coordinate vertices.

The exploration of all of the facets of polyhedral metalloboron cluster chemistry raised in this discussion is continuing in our laboratory.

Experimental Section

Materials. Pentaborane(9) from laboratory stock was purified by trap-to-trap distillation in vacuo. Anhydrous nickel(II) bromide was heated in vacuo before use. Cyclopentadiene was distilled from dicyclopentadiene under a nitrogen atmosphere. Sodium hydride was obtained as a 50% dispersion in mineral oil and used as received. All solvents were reagent grade, and tetrahydrofuran was dried over lithium aluminum hydride before use.

Spectra and Chromatography. ^{11}B and ^1H pulse Fourier transform NMR spectra at 32.1 and 100 MHz, respectively, were recorded on a JEOL PS-100P spectrometer interfaced to a JEOL-Texas Instruments EC-100 computer system. Unit resolution mass spectra were obtained on a Hitachi Perkin-Elmer RMU-6E mass spectrometer, and high-resolution mass measurements were conducted on an AEI MS-902 double-focusing instrument equipped with an SRI chemical ionization source. All high-resolution measurements were performed under chemical ionizing conditions in methane or argon-water. Visible-ultraviolet spectra were obtained on a Cary-14 spectrophotometer, and infrared spectra were recorded on a Beckman IR-8 spectrometer. Thin- and preparative-layer chromatography (TLC) was conducted in air on precoated plates of silica gel F-254 (Brinkmann Instruments, Inc.). Column chromatography was carried out on silica gel (Merck, 70-230 mesh), and high-pressure liquid chromatography was conducted on a Waters Prep/500 chromatograph with 500-mL, 5-cm diameter silica columns under 32 atm radial compression using methylene chloride and methylene chloride-*n*-hexane mixtures as eluents.

All compounds reported herein exhibit strong mass spectroscopic parent groupings with relative intensities consistent with the indicated formulas, and with little evidence of hydrogen loss.

Reaction of $Na^+B_5H_8^-$, $Na^+C_5H_5^-$, and $NiBr_2$. Preparation of 1,7-$(\eta^5\text{-}C_5H_5)_2Ni_2B_{10}H_{10}$ (I) and 1,6-$(\eta^5\text{-}C_5H_5)_2Ni_2B_8H_8$ (II). Freshly distilled cyclopentadiene (11 mmol) and tetrahydrofuran (35 mL) were condensed onto NaH (0.2148 g, 9 mmol) in a 50-mL side-arm flask. Upon warming to room temperature the resulting $Na^+C_5H_5^-$ solution was filtered in vacuo through a glass frit onto a cold (−196 °C) mixture of B_5H_9 (4 mmol) and anhydrous $NiBr_2$ (1.026 g, 5 mmol). The resulting solution was permitted to warm slowly to room temperature with stirring; the color changed from green to brown to black during this period. After room temperature was reached, stirring was continued for another 25 h. After removal of the solvent by distillation in vacuo, the flask was filled with N_2 and removed from the vacuum line. The contents of the flask was extracted with 50-mL portions of hexane and dichloromethane. The combined extracts were placed on a 20-cm silica gel column and eluted with $C_6H_{14}\text{-}CH_2Cl_2$ mixtures of increasing polarity to yield four fractions. These were subsequently subjected to TLC, resulting in the isolation of the following compounds: orange $(C_5H_5)_2Ni_2B_8H_8$, R_f 0.70 (25% CH_2Cl_2 in CCl_4), 3 mg; yellow $(C_5H_5)_2Ni_2B_{10}H_{10}$, R_f 0.36, 10 mg; two trace products which were characterized from mass spectra only, orange $(\sigma\text{-}C_5H_9)\text{-}(C_5H_5)_2Ni_2B_8H_7$, R_f 0.51, 1 mg, and brown $(C_5H_5)_2Ni_2B_{10}H_{10}$ (assumed to be the 1,2 isomer[9c]), R_f 0.12, 1 mg. Exact mass determination for II: calcd for ${}^{60}Ni_2{}^{12}C_{10}{}^{11}B_8{}^1H_{18}^+$ 346.0817, found 346.0800.

Reaction of $Na^+B_5H_8^-$ with Nickelocene. Preparation of $(\eta^5\text{-}C_5H_5)_4Ni_4B_4H_4$ (IV) and $(\eta^5\text{-}C_5H_5)_4Ni_4B_5H_5$ (V). This reaction was run many times in THF under varying conditions. When sodium amalgam was excluded, reaction took place very slowly (if at all), and no $(C_5H_5)_4Ni_4B_4H_4$ or $(C_5H_5)_4Ni_4B_5H_5$ was detected on subsequent workup. When catalytic quantities of sodium amalgam (ca. 0.05 equiv based on nickelocene) were employed, reaction did proceed slowly, but in 12 h at room temperature only traces of the tetranickel clusters were obtained. Therefore, a stoichiometric quantity of sodium is evidently necessary for production of the desired clusters IV and V at a reasonable rate; even then, yields of IV and V varied between ca. 3 and 27% (combined) despite attempts to optimize the reaction conditions. Production of IV and V appears to be adversely affected by the formation of an intractable, air-sensitive, apparently polymeric solid which is insoluble in methylene chloride and other organic solvents; formation of this material is apparently promoted (and yields of IV and V lowered) by trace compounds or other factors not identified. The highest yields (not typical) of IV and V were obtained by the following procedure. Sodium amalgam containing 1.8% sodium by weight was prepared in a 500-mL N_2-filled flask by heating 0.832 g (36 mmol) of freshly cut sodium with 44.801 g of mercury in 12 mL of xylene. Upon formation of the amalgam the mixture was frozen in liquid nitrogen and volatile materials were pumped away. Nickelocene (6.4588 g, 34 mmol) and $Na^+B_5H_8^-$ (23 mmol in 50 mL of THF, prepared from NaH and B_5H_9) were added to the reaction flask. The system was allowed to warm to about −30 °C, at which point hydrogen evolution was observed; the temperature was maintained at −10 to −30 °C for 3 h, after which the mixture was stirred at room temperature overnight. Following removal of solvent in vacuo, the system was exposed to the air, extracted with 500 mL of CH_2Cl_2, and filtered. The filtrate was placed on a silica gel column and eluted with hexane-dichloromethane mixtures; subsequent purification by preparative-scale liquid chromatography on the Prep/500 (35–37% CH_2Cl_2 in *n*-hexane, retention volumes 1050 and 1400 mL, respectively, for IV and V) gave two major products: brown $(C_5H_5)_4Ni_4B_4H_4$ (0.8168 g, 1.506 mmol, 17% yield based on nickel atoms) and green $(C_5H_5)_4Ni_4B_5H_5$ (0.4645 g, 0.838 mmol, 10% yield). Exact masses: for IV, calcd for ${}^{60}Ni_4{}^{12}C_{20}{}^{11}B_4{}^1H_{24}^+$ 547.9578, found 547.9576; for V, calcd for ${}^{60}Ni_4{}^{12}C_{20}{}^{11}B_5{}^1H_{25}^+$ 559.9750, found 559.9743.

A trace of a brown compound with a mass spectrum consistent with the formula $(C_5H_5)_3Ni_3B_7H_8$ was obtained but was not further characterized. 1,7-$(\eta^5\text{-}C_5H_5)_2Ni_2B_{10}H_{10}$ (I) and somewhat larger amounts of 1,6-$(\eta^5\text{-}C_5H_5)_2Ni_2B_8H_8$ (II) were obtained and identified from their mass spectra, R_f values, and ${}^{11}B$ NMR spectra, which matched those of the materials isolated from the $NiBr_2\text{-}B_5H_8^-\text{-}C_5H_5^-$ reaction described above.

Reaction of $Na^+(CH_3)_2C_2B_4H_5^-$ with Nickelocene. Preparation of $(\eta^5\text{-}C_5H_5)_2Ni_2(CH_3)_2C_2B_4H_4$ (VI) and $(\eta^5\text{-}C_5H_5)_2Ni_2(CH_3)_2C_2B_5H_5$ (VII). Sodium amalgam containing 2.1% sodium by weight was prepared by heating 0.2356 g (10.2 mmol) of freshly cut sodium, 11.1427 g of mercury, and 6 mL of xylene in a 100-mL three-neck flask under 500 Torr of dry N_2. Following formation of the amalgam the reaction flask was cooled to −196 °C and volatile materials were removed. The carborane salt $Na^+(CH_3)_2C_2B_4H_5^-$ was prepared separately in a 50-mL side-arm flask by combining NaH (0.3203 g, 13.4 mmol), $(CH_3)_2C_2B_4H_6$ (5.1 mmol),[17] and THF (~20 mL) and warming to room temperature. The resulting solution was passed through a glass frit onto a cold mixture of the amalgam and nickelocene (1.2758 g, 6.7 mmol). The contents of the flask was allowed to warm to −78 °C and stirred for 40 min; following this the solution was warmed to room temperature and stirred overnight. The flask was then opened to the air and the contents filtered; the residue was washed with CH_2Cl_2 and the combined filtrates were stripped of solvent and placed on a silica gel column. Elution with hexane gave primarily green $(C_5H_5)_2Ni_2(CH_3)_2C_2B_4H_4$ (29.0 mg, 3% based on nickel consumed) and brown $(C_5H_5)_2Ni_2(CH_3)_2C_2B_5H_5$ (8.8 mg, 1% yield); further elution with mixtures of CH_2Cl_2 and toluene containing 10–50% CH_2Cl_2 eluted traces of other species whose mass spectra corresponded to C_5H_7- and C_5H_9-substituted derivatives of VI and VII: $(C_5H_5)_2Ni_2(CH_3)_2C_2B_5H_4\text{-}\sigma\text{-}C_5H_7$ (*m/e* 430), $(C_5H_5)_2Ni_2\text{-}(CH_3)_2C_2B_4H_2\text{-}\sigma\text{-}(C_5H_9)_2$ (*m/e* 488), and $(C_5H_5)_2Ni_2(CH_3)_2\text{-}C_2B_4H_3\text{-}\sigma\text{-}C_5H_9$ (*m/e* 420).

X-ray Crystallographic Study of $(\eta^5\text{-}C_5H_5)_4Ni_4B_4H_4$ (IV). A plate-like crystal with maximum dimensions 0.05 × 0.31 × 0.42 mm and having eight indexable faces was selected from several crystals obtained by vapor diffusion of pentane into a methylene chloride solution of the compound, mounted in an arbitrary orientation on a glass fiber, and used for data collection. Crystal data follow: $Ni_4C_{20}B_4H_{24}$, mol wt 542.5, space group $C2/c$, $Z = 4$, $a = 19.546$ (4) Å, $b = 7.512$ (4) Å, $c = 14.86$ (1) Å, $\beta = 106.70$ (2)°, $V = 2090$ (2) Å^3, $\mu(\text{Mo } K\alpha) = 35.3\ \text{cm}^{-1}$, $\rho_c = 1.724\ \text{g cm}^{-3}$, $F(000) = 1104$. For this crystal, the Enraf-Nonius program SEARCH was used to obtain 25 accurately centered reflections which were then used in the program INDEX to obtain an orientation matrix for data collection and to provide approximate cell dimensions. Refined cell dimensions and their estimated standard deviations were obtained from these 25 reflections using the Enraf-Nonius program UNICELL. The mosaicity of the crystal was examined by the ω scan technique and found acceptable. Systematic absences of $h + k = 2n + 1$ on hkl and $l = 2n + 1$ on $h0l$ indicate that the space group is either Cc or $C2/c$. With $Z = 4$, the choice of $C2/c$ requires that the molecule have either twofold or inversion symmetry; the space group was subsequently shown to be $C2/c$ with the molecule bisected by a twofold axis.

Collection and Reduction of the Data. Diffraction data were collected at 295 K on an Enraf-Nonius four-circle CAD-4 diffractometer controlled by a PDP8/M computer, using Mo $K\alpha$ radiation from a highly oriented graphite crystal monochromator. The θ-2θ scan technique was used to record the intensities for all unique reflections for which $1° \leqslant 2\theta \leqslant 52°$. Scan widths were calculated from the formula $SW = A + B \tan\theta$ where A is estimated from the mosaicity of the crystal and B compensates for the increase in the width of the peak due to $K\alpha_1$ and $K\alpha_2$ splitting. The values of A and B were 0.50 and 0.30°, respectively. This calculated scan angle was extended at each side by 25% for background determination (BG1 and BG2). The net count (NC) was then calculated as NC = TOT − 2(BG1 + BG2) where TOT is the estimated peak intensity. Reflection data were considered insignificant for intensities registering less than ten counts above background on a rapid prescan, and these reflections were rejected automatically by the computer. The intensities of three standard reflections were monitored at intervals of 100 reflections and showed no systematic trends. Raw intensity data were corrected for Lorentz-polarization effects which resulted in a total of 1785 intensities of which 1500 had $F_o^2 \geqslant 3\sigma(F_o^2)$, where $\sigma(F_o^2)$ was estimated from counting statistics ($p = 0.03$).[27] Only the latter reflections were used in the final refinement of the structural parameters.

Solution and Refinement of the Structure. The coordinates of the two unique nickel atoms were easily determined from a three-dimensional Patterson map, assuming the space group to be $C2/c$. The Patterson strongly implied $C2/c$ rather than Cc by the presence of Harker sections appropriate for the twofold rotation axis in $C2/c$. Least-squares refinement of the nickel coordinates with isotropic thermal parameters reduced the residuals R and R_w to 0.24 and 0.30, respectively, where residuals are defined as $R = \Sigma||F_o| - |F_c||/\Sigma|F_o|$ and $R_w = (\sigma w(|F_o| - |F_c|)^2/\Sigma w|F_o|^2)^{1/2}$. An electron density difference map phased with the refined nickel positions yielded the locations of all 12 unique carbon and boron atoms. Isotropic followed by anisotropic refinement of all nonhydrogen atoms reduced R to 0.057. An absorption correction was applied to the data (minimum transmission factor 0.735, maximum 0.924) and further refinement reduced R to 0.053. A second electron density difference map yielded the positions of the two hydrogens terminally bonded to boron, after which several cycles of refinement with the hydrogens included with isotropic thermal parameters reduced R to 0.049.

At this point, a careful examination of boron-boron bond lengths as well as some thermal parameters indicated a problem with the data set. An inspection of a list of F_o vs. F_c revealed a small number of reflections with large values for $||F_o| - |F_c||/\sigma(F_o)$. Most of these were collected at virtually the same time, implying some type of transient instrumental difficulty. Elimination of the eight reflections (0.53% of the data) for which $(|F_o| - |F_c|)/\sigma(F_o) > 15$ with subsequent refinement resulted in final values of 0.043 and 0.060 for R and R_w, and the above-mentioned discrepancies in bond lengths and thermal parameters disappeared. During the last cycle of refinement the largest parameter shift was 0.03 times its estimated error. The estimated standard deviation of an observation of unit weight is 2.89 and the data to parameter ratio is 1492/135 = 11.1. The value of R when reflections for which $F_o^2 < 3\sigma(F_o^2)$ are included in the structure factor calculation is 0.06. A final electron density difference map was featureless.

Full-matrix least-squares refinement was based on F, and the function minimized was $\Sigma w(|F_o| - |F_c|)^2$. The weights w were taken as $[2F_o/\sigma(F_o^2)]^2$ where $|F_o|$ and $|F_c|$ are the observed and calculated structure factor amplitudes. The atomic scattering factors for nonhydrogen atoms were taken from Cromer and Waber[28] and those for hydrogen from Stewart.[29] The effects of anomalous dispersion were included in F_c using Cromer and Ibers'[30] values of $\Delta f'$ and $\Delta f''$. The computing system and programs are described elsewhere.[31]

There are no abnormally short intermolecular contacts, the smallest (nonhydrogen) distance being 3.390 (6) Å for C(13)–C(24).

Acknowledgments. This work was supported by the Office of Naval Research and the National Science Foundation, Grant CHE 76-04491. The X-ray diffractometer and associated computing equipment, pulse Fourier transform NMR spectrometer, and preparative-scale high-pressure liquid chromatograph were purchased in part with funds made available through NSF instrumentation grants.

Supplementary Material Available: Listing of observed and calculated structure factors and a table of intermolecular contacts (8 pages). Ordering information is given on any current masthead page.

References and Notes

(1) R. N. Grimes, *Acc. Chem. Res.*, **11**, 420 (1978), and references cited therein.

(2) K. Wade, *Chem. Commun.*, 792 (1971).

(3) (a) K. Wade, *Adv. Inorg. Chem. Radiochem.*, **18**, 1 (1976); (b) R. W. Rudolph, *Acc. Chem. Res.*, **9**, 446 (1976); (c) D. M. P. Mingos, *Nature (London), Phys. Sci.*, **236**, 99 (1972); (d) R. N. Grimes, *Ann. N.Y. Acad. Sci.*, **239**, 180 (1974); (e) R. B. King and D. H. Rouvray, *J. Am. Chem. Soc.*, **99**, 7834 (1977); (f) J. Evans, *J. Chem. Soc., Dalton Trans.*, 18 (1978).

(4) V. R. Miller, R. Weiss, and R. N. Grimes, *J. Am. Chem. Soc.*, **99**, 5646 (1977).

(5) V. R. Miller and R. N. Grimes, *J. Am. Chem. Soc.*, **95**, 5078 (1973); **98**, 1600 (1976).

(6) (a) J. R. Pipal and R. N. Grimes, *Inorg. Chem.*, **16**, 3255 (1977); (b) *ibid.*, **18**, 252 (1979); (c) *ibid.*, **18**, 257 (1979).

(7) (a) R. Weiss and R. N. Grimes, *J. Am. Chem. Soc.*, **99**, 8087 (1977); (b) *Inorg. Chem.*, in press.

(8) J. R. Bowser and R. N. Grimes, *J. Am. Chem. Soc.*, **100**, 4623 (1978).

(9) (a) B. P. Sullivan, R. N. Leyden, and M. F. Hawthorne, *J. Am. Chem. Soc.*, **97**, 455 (1975); (b) R. N. Leyden and M. F. Hawthorne, *J. Chem. Soc., Chem. Commun.*, 310 (1975); (c) R. N. Leyden, B. P. Sullivan, R. T. Baker, and M. F. Hawthorne, *J. Am. Chem. Soc.*, **100**, 3758 (1978).

(10) (a) V. R. Miller and R. N. Grimes, *J. Am. Chem. Soc.*, **95**, 2830 (1973); (b) W. J. Evans, G. B. Dunks, and M. F. Hawthorne, *ibid.*, **95**, 4565 (1973).

(11) The only other reported metal–boron cage structure containing a metal–metal distance shorter than 2.40 Å is that of icosahedral $(C_5H_5)_2Co_2C_2B_8H_{10}$ [2.387 (2) Å].[12] It should be pointed out that no structure determinations are available for eight-vertex metalloboron systems other than $(\eta^5\text{-}C_5H_5)_4M_4B_4H_4$ (M = Co, Ni); comparisons of metal–metal distances among different classes of polyhedra are complicated by possible geometric constraints and by varying coordination environments of the metal atoms. Nevertheless, the fact remains that the metal–metal distances in IV are significantly shorter than any others yet found in a metal–boron cage.

(12) K. P. Callahan, C. E. Strouse, A. L. Sims, and M. F. Hawthorne, *Inorg. Chem.*, **13**, 1397 (1974).

(13) (a) G. Longoni, P. Chini, L. D. Lower, and L. F. Dahl, *J. Am. Chem. Soc.*, **97**, 5034 (1975); (b) J. K. Ruff, R. P. White, Jr., and L. F. Dahl, *ibid.*, **93**, 2159 (1971), and references cited therein; (c) O. S. Mills and B. W. Shaw, *J. Organomet. Chem.*, **11**, 595 (1968).

(14) Private communication from Dr. A. J. Welch, New University of Ulster, Londonderry, Northern Ireland. We thank Dr. Welch for informing us of these results prior to publication.

(15) C. G. Salentine, C. E. Strouse, and M. F. Hawthorne, *Inorg. Chem.*, **15**, 1832 (1976).

(16) R. N. Grimes in "Organometallic Reactions and Syntheses", Vol. 6, E. I. Becker and M. Tsutsui, Eds., Plenum Press, New York, 1977, Chapter 2, and references cited therein.

(17) T. Onak and G. B. Dunks, *Inorg. Chem.*, **5**, 439 (1966).

(18) L. Venable and R. N. Grimes, unpublished results.

(19) G. K. Barker, M. Green, J. L. Spencer, F. G. A. Stone, B. F. Taylor, and A. J. Welch, *J. Chem. Soc., Chem. Commun.*, 804 (1975); (b) V. R. Miller, L. G. Sneddon, D. C. Beer, and R. N. Grimes, *J. Am. Chem. Soc.*, **96**, 3090 (1974); (c) V. R. Miller and R. N. Grimes, *ibid.*, **97**, 4213 (1975); (d) C. G. Salentine and M. F. Hawthorne, *ibid.*, **97**, 6382 (1975); (e) K. P. Callahan, W. J. Evans, F. Y. Lo, C. E. Strouse, and M. F. Hawthorne, *ibid.*, **97**, 296 (1975); (f) W. M. Maxwell, V. R. Miller, and R. N. Grimes, *ibid.*, **98**, 4818 (1976); (g) *Inorg. Chem.*, **15**, 1343 (1976); (h) W. M. Maxwell, K-S. Wong, and R. N. Grimes, *ibid.*, **16**, 3094 (1977); (i) E. L. Hoel, C. E. Strouse, and M. F. Hawthorne, *ibid.*, **13**, 1388 (1974); (j) W. J. Evans and M. F. Hawthorne, *ibid.*, **13**, 869 (1974); (k) K. P. Callahan, C. E. Strouse, A. L. Sims, and M. F. Hawthorne, *ibid.*, **13**, 1397 (1974); (m) R. N. Grimes, A. Zalkin, and W. T. Robinson, *ibid.*, **15**, 2274 (1976).

(20) L. J. Guggenberger, *Inorg. Chem.*, **8**, 2271 (1969).

(21) H. Hart and W. N. Lipscomb, *Inorg. Chem.*, **7**, 1070 (1968).

(22) (a) G. S. Pawley, *Acta Crystallogr.*, **20**, 631 (1966); (b) R. A. Jacobson and W. N. Lipscomb, *J. Chem. Phys.*, **31**, 605 (1959); (c) R. A. Jacobson and W. N. Lipscomb, *J. Am. Chem. Soc.*, **80**, 5571 (1958).

(23) (a) E. L. Muetterties and B. F. Beier, *Bull. Soc. Chim. Belg.*, **84**, 397 (1975); (b) J. Evans, *J. Chem. Soc., Dalton Trans.*, 18 (1978); (c) E. L. Muetterties, R. J. Wiersema, and M. F. Hawthorne, *J. Am. Chem. Soc.*, **95**, 7520 (1973).

(24) T. P. Fehlner, *J. Am. Chem. Soc.*, **99**, 8355 (1977).

(25) (a) M. K. Kaloustian, R. J. Wiersema, and M. F. Hawthorne, *J. Am. Chem. Soc.*, **94**, 6679 (1972); (b) D. F. Dustin, W. J. Evans, C. J. Jones, R. J. Wiersema, H. Gong, S. Chan, and M. F. Hawthorne, *ibid.*, **96**, 3085 (1974); (c) W. J. Evans, C. J. Jones, B. Stibr, and M. F. Hawthorne, *J. Organomet. Chem.*, **60**, C27 (1973); (d) V. R. Miller and R. N. Grimes, *J. Am. Chem. Soc.*, **97**, 4213 (1975); (e) W. M. Maxwell, R. Weiss, E. Sinn, and R. N. Grimes, *ibid.*, **99**, 4016 (1977).

(26) Additional isomers may exist; however, any such species in the cobalt and nickel reaction systems discussed herein would have to be present in quantities far smaller than the characterized isomers to escape detection. No evidence of isomers of the tetrametallic clusters has been observed.

(27) P. W. R. Corfield, R. J. Doedens, and J. A. Ibers, *Inorg. Chem.*, **6**, 197 (1967).

(28) D. T. Cromer and J. R. Waber, "International Tables for X-ray Crystallography", Vol. IV, Kynoch Press, Birmingham, England, 1974.

(29) R. F. Stewart, E. R. Davidson, and W. T. Simpson, *J. Chem. Phys.*, **42**, 3175 (1965).

(30) D. T. Cromer and J. A. Ibers, ref 27.

(31) D. P. Freyberg, G. M. Mockler, and E. Sinn, *J. Chem. Soc., Dalton Trans.*, 447 (1976).